

Unique Phase Recovery for Nonperiodic Objects

K. A. Nugent,¹ A. G. Peele,¹ H. N. Chapman,² and A. P. Mancuso¹

¹*School of Physics, The University of Melbourne, Victoria, 3010, Australia*

²*Lawrence Livermore National Laboratory, PO Box 808, Livermore, California 94450, USA*

(Received 2 April 2003; published 13 November 2003)

It is well known that the loss of phase information at detection means that a diffraction pattern may be consistent with a multitude of physically different structures. This Letter shows that it is possible to perform unique structural determination in the absence of *a priori* information using x-ray fields with phase curvature. We argue that significant phase curvature is already available using modern x-ray optics and we demonstrate an algorithm that allows the phase to be recovered uniquely and reliably.

DOI: 10.1103/PhysRevLett.91.203902

PACS numbers: 42.30.Rx, 41.50.+h, 61.10.Nz, 87.10.+e

Since the discovery of the laws describing the diffraction of x rays by crystals, x-ray diffraction has played a pivotal role in developing an understanding of the physics of materials and is a central technique of modern structural biology. The development of very high-brightness x-ray sources, such as third-generation synchrotron sources, enables diffraction data to be acquired from ever-smaller samples. The loss of phase information at measurement may be compensated by introducing additional information via, for example, atomicity assumptions in direct methods [1], structural substitution methods [2], and single or multiple anomalous dispersion methods [3]. The development of x-ray free-electron lasers promises the acquisition of diffraction data from very small crystals or even single molecules [4], and recent work by Miao *et al.* [5] has demonstrated the reconstruction of such noncrystallographic specimens from diffraction data, although the uniqueness of the reconstruction cannot be guaranteed. Unique real-space phase recovery methods have been demonstrated and successfully applied [6] but have hitherto been thought to fail in the far-field limit. In this paper we consider the real-space ideas in the context of the diffraction of fields containing cylindrical phase curvature, which we term astigmatic fields. We show that astigmatic diffraction patterns allow unique recovery of structural information from diffracted intensities in reciprocal space.

The diffraction imaging work of Miao *et al.* [5], following on from the ideas of Sayre and colleagues [7], recovers a wave field from its diffracted intensities using the so-called oversampling method. Fourier methods tell us that a complete reconstruction of an object may be obtained from reciprocal space samples taken at intervals specified by the Nyquist condition. The oversampling approach posits that reciprocal space data should be sampled at a greater rate since the additional data contain information about the object “support”—a region of real space known to fully contain the object. It is further posited that incorporating support information greatly reduces the possible data sets consistent with the diffracted intensity, and it is observed that the recovered solution is often the correct one. Indeed, it has been

shown that knowledge of the support associated with the diffracted intensities almost always enables a unique phase recovery, given a degree of oversampling [8]. The structure is found using iterative methods based on the original Gerchberg-Saxton approach as modified by Fienup [9].

Recent work has shown that noninterferometric phase recovery is possible in real space for x rays [10], along with other forms of waves [6]. Noninterferometric real-space phase recovery methods depend on the fact that the evolution of the intensity with propagation carries phase information through curvature in the diffracted wave. However, the far field is precisely that region where curvature is negligible. In the far field, the intensity distribution merely expands on propagation and so all propagation-based phase information is lost. In the work described here, the curvature is reintroduced by considering a nonplanar incident field.

Suppose a coherent x-ray wave, $\psi_{\text{inc}}(\vec{r}, z)$, where \vec{r} is a two-dimensional vector, strikes a finite sample and produces a diffracted wave ψ_{diff} . The sample is assumed to be sufficiently small so that the diffracted field is detected in the far field and its diffracting properties are contained in its 3D scattering potential, $V(\vec{r}, z)$. In the far field, $\psi_{\text{diff}}(\vec{r}, z) \rightarrow \psi_{\text{diff}}(r\vec{\rho})$, where r is the distance of the observation point from the detector point, $(\rho_x, \rho_y, \sqrt{1 - \rho_x^2 - \rho_y^2})$ is the unit vector in the direction of propagation, and we define $\vec{\rho} \equiv (\rho_x, \rho_y)$. As a very small sample will only diffract x rays weakly, we adopt the Born approximation so that the diffracted wave is described by

$$\psi_{\text{diff}}(r\vec{\rho}) \approx \psi_{\text{inc}}(r\vec{\rho}) + \psi_f(r\vec{\rho}), \quad (1)$$

where [11]

$$\begin{aligned} \psi_f(r\vec{\rho}) = & -ik_0^2 \frac{e^{ik_0 r}}{r} \\ & \times \int \psi_{\text{inc}}(\vec{r}', z') V(\vec{r}', z') e^{-ik_0[\vec{\rho}\vec{r}' + z'\sqrt{1-\rho^2}]} d\vec{r}' dz', \end{aligned} \quad (2)$$

where $k_0 = 2\pi/\lambda$, and λ is the wavelength. In the

remaining discussion we consider only the angular component, $U_f(\vec{\rho})$ of the far-field distribution, where $U_f(\vec{\rho})$ is defined via $\psi_f(r\vec{\rho}) = U_f(\vec{\rho})(e^{ik_0 r}/r)$.

We now suppose that a phase change $\alpha(\vec{r})$ is introduced onto an initially planar incident field. In this case,

$$\psi_{\text{inc}}(\vec{r}) = e^{i[\alpha(\vec{r}) - k_0 z]} \approx e^{-ik_0 z}[1 + i\alpha(\vec{r})], \quad (3)$$

where we note that modern x-ray optics will produce only a small phase change across its focal region and so assume that the phase curvature is small. We also assume that the object is sufficiently small so that $\alpha(\vec{r})$ can be considered not to vary through the structure—it has no z dependence. We may then write the far-field wave in terms of the diffracted wave with zero incident curvature, $U_f^0(\vec{\rho})$ as

$$U_f(\vec{\rho}) = U_f^0(\vec{\rho}) + i\chi(\vec{\rho}), \quad (4)$$

where

$$\chi(\vec{\rho}) \equiv -ik_0^2 \int \alpha(\vec{r}') V(\vec{r}', z') e^{-ik_0[\vec{\rho}\vec{r}' - z'(-1 + \sqrt{1 - \rho^2})]} d\vec{r}' dz'. \quad (5)$$

The modified far-field scattered intensity is therefore

$$I_f'(\vec{\rho}) \approx I_f(\vec{\rho}) + i\{U_f^{0*}(\vec{\rho})\chi(\vec{\rho}) - U_f^0(\vec{\rho})\chi^*(\vec{\rho})\}, \quad (6)$$

where the second order terms in $\chi(\vec{\rho})$ have been ignored and $I_f(\vec{\rho}) \equiv |U_f^0(\vec{\rho})|^2$.

We now consider the specific case of the introduction of a small additional parabolic phase change $\alpha(\vec{r}) = (k_0 r^2/2R)$ into an otherwise conventional diffraction experiment. R is the characteristic scale of the phase change. In modern x-ray optics, the paraxial limit is appropriate in describing the incident field, in which case R becomes the radius of curvature of an incident spherical wave. Following Eq. (3), the illuminating wave may therefore be written $\psi_{\text{inc}}(\vec{r}) \approx [1 + ik_0(r^2/2R)]e^{-ik_0 z}$.

We now make the projection approximation, which assumes that the object is sufficiently thin so that the z' dependence may be ignored. This requires that the width of the object in the z direction, δz , obeys the condition $\delta z \ll 1/k_0 \rho_{\text{max}}^2$, where ρ_{max} is the maximum lateral spatial frequency measured [12]. Using Eq. (5), we then find

$$\chi(\vec{\rho}) = -\frac{1}{2k_0 R} \nabla^2 U_f^0(\vec{\rho}), \quad (7)$$

so that Eq. (6) may be rewritten:

$$I_f'(\vec{\rho}) \approx I_f(\vec{\rho}) + \frac{1}{2k_0 R} i\{U_f^0(\vec{\rho}) \nabla^2 U_f^{0*}(\vec{\rho}) - U_f^{0*}(\vec{\rho}) \nabla^2 U_f^0(\vec{\rho})\}. \quad (8)$$

This may, in turn, be written in the form

$$I_f'(\vec{\rho}) \approx I_f(\vec{\rho}) + \frac{1}{k_0 R} \nabla\{I_f(\vec{\rho}) \nabla \Phi_f(\vec{\rho})\}. \quad (9)$$

Here we have introduced the definition $U_f^0(\vec{\rho}) \equiv \sqrt{I_f(\vec{\rho})} e^{i\Phi_f(\vec{\rho})}$, where Φ_f contains the diffracted phase information. If we define $\delta I_f(\vec{\rho}) \equiv I_f(\vec{\rho}) - I_f'(\vec{\rho})$ then

$$k_0 R \delta I_f(\vec{\rho}) = \nabla\{I_f(\vec{\rho}) \nabla \Phi_f(\vec{\rho})\}. \quad (10)$$

This has a structure that is formally identical to the transport of the intensity equation [13] used in real-space phase determination. However it is important to realize that this expression is fundamentally different: it does not assume paraxiality and it describes a field in reciprocal space.

In the context of the Neuman problem [14], Eq. (10) has a unique solution given knowledge of the boundary condition $\vec{n} \nabla \Phi_f = g$, where $\vec{n} \nabla \Phi_f$ is the phase gradient normal to the boundary, and $I_f(\vec{\rho}) > 0$ over a simply connected bounded two-dimensional domain. Unfortunately, these uniqueness conditions are violated for most diffracted fields. In particular, phase discontinuities are almost inevitably associated with zeros in the intensity and Eq. (10) will rarely yield a unique solution.

At a deep level, the phase ambiguity arises from the symmetries buried in the phase discontinuity structure [15] and so might be expected to be broken by the introduction of an asymmetric optical system. Consider, then, illuminating the sample with a cylindrical, rather than spherical, wave. In this case the phase distribution is described by

$$\alpha(x, y) = \frac{k_0}{2R} x^2. \quad (11)$$

An entirely analogous argument to that given before leads to the expression:

$$k_0 R \delta I_f(\vec{\rho}) \approx \partial_{\rho_x} \{I_f(\vec{\rho}) \partial_{\rho_x} \Phi_f(\vec{\rho})\}, \quad (12)$$

where $\partial_{\rho_x} \Phi_f(\vec{\rho})$ is the partial derivative of $\Phi_f(\vec{\rho})$ in the ρ_x direction.

The Poynting vector for a coherent optical field with intensity I and phase Φ has the form $\vec{S}(\vec{r}) = (1/k_0) I(\vec{r}) \nabla \Phi(\vec{r})$. Equation (12) has the property that it allows the x component of the Poynting vector $(1/k_0) I_f(\vec{\rho}) \partial_{\rho_x} \Phi_f(\vec{\rho})$ to be directly obtained, to within an arbitrary function of ρ_y :

$$\frac{1}{k_0} I_f(\vec{\rho}) \partial_{\rho_x} \Phi_f(\vec{\rho}) = R \int \delta I_f(\vec{\rho}) d\rho_x + g_x(\rho_y). \quad (13)$$

Neuman boundary conditions may now be introduced. We assume, for the purposes of this argument, that the boundary Γ is rectangular so that $\vec{n} \nabla \Phi_f|_{\Gamma} = \partial_{\rho_x} \Phi_f|_{\Gamma}$ is known along the boundary. In practice, we may often assume that the object is fully contained within Γ so that the boundary condition requires that the Poynting vector vanishes at Γ . In this way, $g_x(\rho_y)$ can be obtained and $(1/k_0) I_f(\vec{\rho}) \partial_{\rho_x} \Phi_f(\vec{\rho})$ is fully determined. If the y curvature is also introduced, the same process can be applied to recover $(1/k_0) I_f(\vec{\rho}) \partial_{\rho_y} \Phi_f(\vec{\rho})$. Thus the

Poynting vector field $(1/k_0)I_f(\vec{\rho})\nabla\Phi_f(\vec{\rho})$ is uniquely determined.

It is straightforward to see that the Poynting vector field uniquely specifies the phase of the coherent field to within a physically meaningless constant [16]. Methods exist for the direct integration of $\nabla\Phi_f(\vec{\rho})$ to recover the phase distribution, given suitable care in the treatment of phase vortices [17]. We are therefore able to conclude that a measurement of the far-field diffraction pattern combined with far-field diffraction patterns obtained with orthogonal cylindrically curved waves is sufficient to *uniquely* determine the phase of the diffraction pattern. This is the central result of this Letter. As the proposed method uses astigmatic optical elements to illuminate the sample, we refer to the method as *astigmatic diffraction*.

Although it would be possible to directly integrate a Poynting vector field to recover the phase distribution, a diffracted field will typically contain many vortices and so this will, in general, not be practical. We therefore developed an iterative scheme to solve for the phase. The algorithm is similar in spirit to other iterative methods [9] and commenced with a phase guess (either uniform or random initial guesses were used) and uniform intensity. The algorithm is described in Fig. 1, but the essential idea is to iterate between the three diffraction data sets and to impose the measured diffracted intensities at each incident phase curvature while letting the phase arrive at a consistent set of values. The argument in this paper proves that a consistent phase distribution is uniquely specified as the correct one.

In order to assist with convergence, a loose support constraint was used to correct the data in real space. In the simulations here, the support required that the object have a maximum linear extent not exceeding half that of the reconstructed field of view. This corresponds to an oversampling ratio [5] of 4, though we have found convergence also occurs with a lower oversampling ratio. With this rather weak support constraint, we found that the algorithm always quickly found the unique solution. In order to assess convergence, we define a quality of fit parameter against the correct solution, determined over the support:

$$R \equiv \sum_{i,j} \left| \left| d_{ij}^{\text{recon}} \right| - \left| d_{ij}^{\text{truth}} \right| \right| / \sum_{i,j} \left| \left| d_{ij}^{\text{recon}} \right| + \left| d_{ij}^{\text{truth}} \right| \right|, \quad (15)$$

where d_{ij}^{recon} is the i th pixel of the reconstruction and d_{ij}^{truth} is the corresponding correct value.

A principal application of the method lies in its application to small crystal diffraction [18]. In order to explore that application, the diffraction pattern from a nanocrystal of lysozyme molecules was simulated without approximation. This molecule has a unit cell of $38.07 \times 33.20 \times 46.12$ Å. Diffraction of x rays with a wavelength of 1.5 Å from a $3 \times 3 \times 3$ nanocrystal was

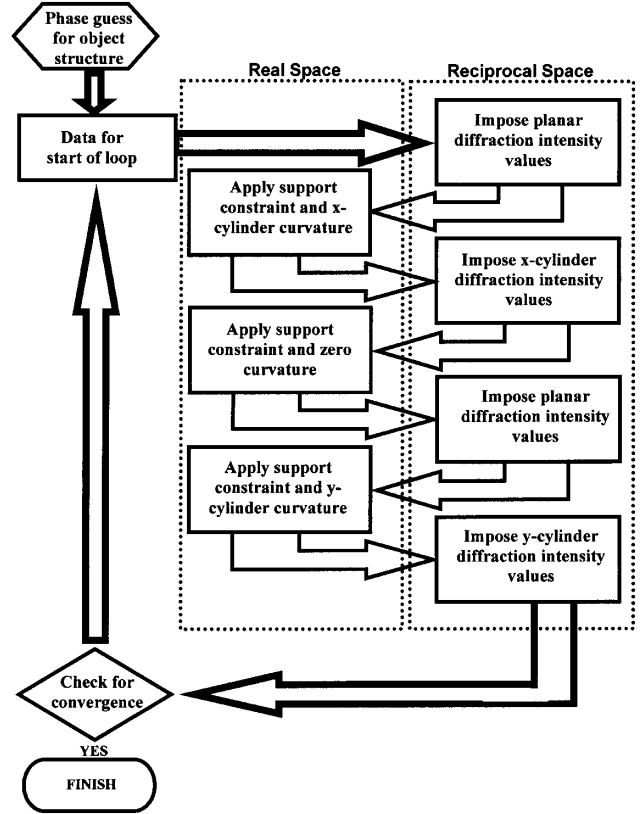


FIG. 1. Outline of the algorithm to recover the phase from astigmatic diffraction data. The algorithm uses diffracted intensities from a planar incident field and cylindrically curved fields in the x and y directions. It then iteratively seeks a phase distribution consistent with the intensity data using a form of the Fienup hybrid input-output algorithm. The algorithm cycles between real (i.e., sample) space and Fourier (i.e., detector) space for each of the incident fields. It imposes the measured intensities in Fourier space and imposes a finite support constraint in real space while leaving the phase free to find a set of values consistent with the measurement. Once the algorithm begins to converge, it is found that the rate of convergence is improved by removing the support constraint altogether.

simulated. Note that, for this example, the projection approximation leading to Eq. (7) implies a resolution limit for the method of about 6 Å. The diffraction pattern was calculated for a planar wave and the magnitude of the correct diffracted field amplitude at the molecule is shown in Fig. 2(a). Diffraction patterns were calculated using illumination with a moderate cylindrical curvature in both the x and the y directions (maximum phase excursion of 1.3π). The algorithm given in Fig. 1 was then applied to the data with the result shown in Fig. 2(b). This reconstruction has $R = 12.5 \times 10^{-2}$.

Comparisons were made with the reconstruction using a Fienup-type hybrid input-output algorithm. As might be expected [8], the Fienup approach produces a visually acceptable, but inferior, recovery ($R = 31.5 \times 10^{-2}$), but required a very tight support constraint containing detailed object shape information.

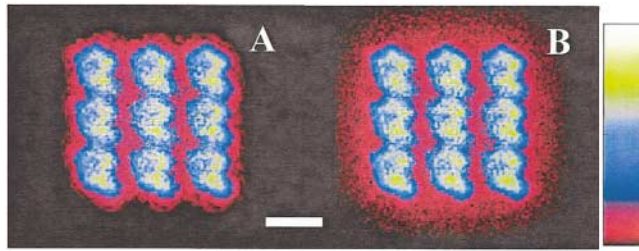


FIG. 2 (color). Reconstructions using the iterative algorithm. (a) The correct magnitude of the field diffracted by the lysozyme molecule. (b) Magnitude of the reconstruction of the diffracted amplitude using the astigmatic diffraction technique. The agreement with the field shown in (a) is excellent. The scale bar is 40 Å in length.

When coherently illuminated, modern zone plates can deliver diffraction limited focal spot sizes of around 100 nm for harder x rays [19], and 30 nm or better [20] for softer x rays. These zone plates have a diameter of around 100 μm , and significant levels of coherence have been observed on these length scales [21] confirming that diffraction limited focal spots are achievable. This argument suggests that it should be possible to uniquely phase diffracted data from crystal structures with a unit cell with a size > 30 nm using already existing technology, which brings the method into the range of moderate sized protein crystals. We also note that there has been recent work in diffractive optical elements [22] that will have the potential to develop novel x-ray wave fronts that may find application to methods such as that discussed here.

In this Letter we have developed a theoretical formalism that will allow structural information to be extracted uniquely without detailed knowledge of the object shape. The algorithm we have developed converges reliably and rapidly, with results that are better than are achieved using methods depending on *a priori* shape information. The diffraction data are acquired using x-ray optical elements with requirements that are within the current state of the art. We therefore believe that this method is a reliable new approach to directly and uniquely recovering the structures of nonperiodic samples. The method should immediately find a role in structural studies of both small crystals and in the high resolution imaging of biological structures.

K. A. N., A. G. P., and A. P. M. acknowledge support of the Australian Research Council. This work was partly performed under the auspices of the U.S. DOE by LLNL under Contract No. W-7405-ENG-48.

- [1] See, e.g., H. Hauptman and J. Karle, *The Solution of the Phase Problem I. The Centrosymmetric Crystal*, American Crystallographic Association Monograph Vol. 3 (Polycrystal Book Service, Pittsburgh, PA, 1953).
- [2] T. L. Blundell and L. N. Johnson, *Protein Crystallography* (Academic, London, 1976).
- [3] W. A. Hendrickson, *Science* **254**, 51–58 (1991).
- [4] R. Neutze, R. Wouts, D. van der Spoel, E. Weckert, and J. Hajdu, *Nature* (London) **406**, 752–757 (2000).
- [5] J. W. Miao, P. Charalambous, J. Kirz, and D. Sayre, *Nature* (London) **400**, 342–344 (1999).
- [6] D. Paganin and K. A. Nugent, *Adv. Imag. Electron Phys.* **118**, 85–127 (2001).
- [7] D. Sayre and H. N. Chapman, *Acta Crystallogr. Sect. A* **51**, 237–252 (1995).
- [8] R. H. T. Bates, *Optik* **61**, 247–262 (1982).
- [9] J. R. Fienup, *Appl. Opt.* **21**, 2758–2769 (1982).
- [10] K. A. Nugent, T. E. Gureyev, D. F. Cookson, D. Paganin, and Z. Barnea, *Phys. Rev. Lett.* **77**, 2961–2964 (1996).
- [11] L. Mandel and E. Wolf, *Optical Coherence and Quantum Optics* (Cambridge University Press, Cambridge, 1995), pp. 125–127.
- [12] Scattering from a three-dimensional object will mean that it is difficult to properly define an appropriate support constraint for such objects. The limitation identified here also has an analog in methods requiring well-specified *a priori* support information.
- [13] M. R. Teague, *J. Opt. Soc. Am.* **73**, 1434–1441 (1983).
- [14] T. E. Gureyev, A. Roberts, and K. A. Nugent, *J. Opt. Soc. Am. A* **12**, 1942–1946 (1995).
- [15] K. A. Nugent and D. Paganin, *Phys. Rev. A* **61**, 063614 (2000).
- [16] Consider two waves with the same intensity distribution but different phases $\Phi_1(\vec{\rho})$ and $\Phi_2(\vec{\rho})$. The demand that the two Poynting vectors be the same is written $I_F(\vec{\rho})\{\nabla[\Phi_1(\vec{\rho}) - \Phi_2(\vec{\rho})]\} = 0$. Thus $\Phi_1(\vec{\rho}) - \Phi_2(\vec{\rho}) = \text{const}$.
- [17] V. P. Aksenov and O. V. Tikhomirova, *J. Opt. Soc. Am. A* **19**, 345–355 (2002).
- [18] I. A. Vartanyants and I. K. Robinson, *J. Phys. Condens. Matter* **13**, 10593–10611 (2001).
- [19] Hard x-ray zone plates with a resolution of better than 100 nm are available commercially. See http://www.xradia.com/pro_zpl.htm
- [20] E. H. Anderson, D. L. Olynick, B. Harteneck, E. Veklerov, G. Denbeaux, W. Chao, A. Lucero, L. Johnson, and D. Attwood, *J. Vac. Sci. Technol. B* **18**, 2970–2975 (2000).
- [21] D. Paterson, B. E. Allman, P. J. McMahon, J. Lin, N. Moldovan, K. A. Nugent, I. McNulty, C. T. Chantler, C. C. Retsch, T. H. K. Irving, and D. C. Mancini, *Opt. Commun.* **195**, 79–84 (2001).
- [22] A. A. Firsov, A. A. Svintsov, S. I. Zaitsev, A. Erko, and V. V. Aristov, *Opt. Commun.* **202**, 55–59 (2002).